Research Square

Preprints are preliminary reports that have not undergone peer review.
They should not be considered conclusive, used to inform clinical practice,
or referenced by the media as validated information.

Expanding *DYSF* Mutational Landscape: Identification of Novel Variants associated with Limb-Girdle Muscular Dystrophy Type R2

Yasin Zerafat
Shiraz University of Medical Sciences
Maryam Fazelzadeh Haghighi
Shiraz University of Medical Sciences
Zahra Farbood
Shiraz University of Medical Sciences
Fatemeh Jalali
Shiraz University of Medical Sciences
Elnaz Khosravian
Shiraz University of Medical Sciences
Jafar Mehrabi Sisakht
mehrabisj@gmail.com

Shiraz University of Medical Sciences

Research Article

Keywords: WES, Dysferlinopathy, DYSF gene, LGMD

Posted Date: September 21st, 2026

DOI: https://doi.org/10.21203/rs.3.rs-10677014/v1

License: This work is licensed under a Creative Commons Attribution 4.0 International License. Read Full License

Additional Declarations: No competing interests reported.

Abstract

Background

Dysferlinopathy is a clinically and genetically heterogeneous group of muscular dystrophies caused by pathogenic variants in the *DYSF* gene, most commonly presenting as limb-girdle muscular dystrophy type R2. Given the marked phenotypic variability, molecular genetic testing is essential for accurate diagnosis.

Methods

Two unrelated consanguineous families with adult-onset, progressive proximal muscle weakness and markedly elevated serum creatine kinase levels were clinically evaluated. Whole-exome sequencing was performed to identify the underlying genetic cause.

Results

WES revealed two novel homozygous truncating *DYSF* variants. A nonsense variant (c.5404G > T; p.Glu1802*) in exon 47 was identified in the first family, while a frameshift insertion (c.2755_2756insC; p.Tyr919Serfs*6) in exon 26 was detected in the second family. Both variants were absent from population databases, showed complete co-segregation with disease, and were classified as pathogenic according to ACMG criteria. In silico and structural analyses predicted severe disruption of dysferlin protein function.

Conclusion

These findings expand the mutational spectrum of *DYSF* and highlight the value of WES for diagnosing dysferlinopathy, particularly in consanguineous populations, with important implications for genetic counselling.

Background

A clinically and genetically varied group of neuromuscular disorders known as limb-girdle muscular dystrophies (LGMDs) are characterized by a gradual weakening of the shoulder and pelvic muscles. One of the most prevalent subtypes in the autosomal recessive category is dysferlinopathy, which is brought on by damaging mutations in the *DYSF* gene [1]. The *DYSF* gene produces dysferlin, a membrane-linked protein necessary for sarcolemma repair; its loss of function causes persistent inflammation and degeneration of muscle fibers. Miyoshi distal myopathy and limb-girdle muscular dystrophy type R2 (LGMDR2) are two examples of the clinical spectrum's wide range, which frequently makes early diagnosis difficult [2].

Our ability to identify *DYSF* mutations has been greatly enhanced by NGS technologies, which have also increased our understanding of the associated genotypic and phenotypic variation [3]. The need for thorough clinical and genetic characterization of affected families is highlighted by the fact that patients with various *DYSF* mutations continue to show notable variation in sickness severity, onset timing, and disease history [4].

This paper presents the results of two unrelated families with limb-girdle muscular dystrophy caused by pathogenic mutations in *DYSF* that have not yet been described. We investigate genotype-phenotype correlations and add to the growing list of mutations linked to dysferlinopathy through thorough clinical examination and Whole-exome sequencing (WES).

Methods

Clinical Evaluation

Every person with the dystrophy from both families underwent a thorough clinical evaluation, including neurological evaluation, measurement of serum CK, and documentation of the start and course of the illness. When possible, electromyography (EMG) examination was carried out. Family medical histories were gathered through structured interviews, and pedigree charts were made using web-based pedigree construction software.

DNA Extraction

Tubes containing EDTA were used to collect a blood sample. Using the Pishgam DNA Extraction Kit (Pishgam, Iran) and the manufacturer's instructions, we extracted genomic DNA from white blood cells. NanoDrop spectrophotometry was used to assess the quantity and quality of DNA.

WES

Affected individuals underwent WES, using the NovaSeq 6000 SBS Kit (Illumina). The building of the library followed conventional Illumina procedures. The goal of paired-end sequencing was to achieve a mean coverage of more than 100× [3].

Bioinformatic Analysis

The bioinformatic analysis started by evaluating the quality of raw FASTQ, using FastQC and trimming low-quality bases with Trimmomatic. High-quality reads were aligned to the human reference genome (GRCh38/hg38) using BWA, and the resulting BAM files were sorted and deduplicated with SAMtools and Picard. Variant calling was performed with GATK HaplotypeCaller, followed by quality filtering using GATK VariantFiltration and VCFtools. Functional annotation of high-confidence variants was carried out using ANNOVAR and VEP, and annotated variants were exported to Excel for manual inspection [5].

The variants were first filtered by population allele frequency using gnomAD, the 1000 Genomes Project, and HapMap, retaining only rare or novel variants. Additional filtering steps incorporated gene function, predicted molecular impact, expected inheritance pattern, and compatibility with the clinical phenotype. A multistep variant-prioritization pipeline was then applied. Remaining candidates were evaluated using multiple pathogenicity prediction tools (CADD, SIFT, PolyPhen-2, M-CAP, REVEL) and classified according to ACMG/AMP guidelines, with cross-referencing to ClinVar, HGMD, and OMIM. This workflow narrowed the results to a single likely pathogenic variant in each family, which was validated by Sanger sequencing and confirmed through co-segregation analysis [6].

To further ensure reliability, we visually inspected aligned reads using IGV; also, given the known contribution of structural variants to dysferlinopathy, CNV analysis was performed using Conifer and ExomeDepth to screen for potential *DYSF* deletions or duplications not detectable by standard variant-calling pipelines [7, 8].

Variant Interpretation

Every detected *DYSF* gene variant was assessed using the American College of Medical Genetics and Genomics (ACMG) standards. The assessment criteria included previously recognized illness associations, familial segregation

patterns, population frequency, and computational pathogenicity forecasts. The zygosity status (homozygous or compound heterozygous) of each affected individual was ascertained [9].

Results

Clinical Description of Families

We investigated two unrelated consanguineous families with a history of progressive muscle weakness consistent with autosomal recessive limb-girdle muscular dystrophy (LGMDR2).

Family 1

The 30-year-old female index patient (IV-3, Fig. 1) first experienced symptoms when she was about 25 years old. Gradually, the disease worsened to the point that substantial proximal muscle weakness required ambulatory assistance. Similar gradual weakness and obvious muscle atrophy were shown by her afflicted brother (IV-2). Serum CK (2509 IU/L), AST, and ALT values were significantly high, according to laboratory testing. (Fig. 1)

Family 2

The 33-year-old male index patient (IV-4, Fig. 2), who was born to consanguineous parents, first experienced symptoms between the ages of 25 and 26. He had minor gait impairment, progressively worsening proximal muscular weakness, and trouble getting up from the floor and climbing stairs. The physical examination revealed proximal muscle involvement, decreased muscular tone, and a positive Gowers' sign. Elevated levels of CK (4300 IU/L) and LDH (756 IU/L) were found by laboratory testing. His sister (IV-3) had the same illness, but it had progressed to the point where she needed wheelchair help. EMG revealed a considerable myopathic process in all examined muscles, with proximal muscles being most impacted. (Fig. 2)

Genetic Findings and Variant Classification

Family 1: Nonsense Variant (p.Glu1802*)

A homozygous nonsense mutation in *DYSF*, located in exon 47 (c.5404G > T; p.Glu1802*), was discovered by WES. It is anticipated that this mutation will prevent normal dysferlin function by introducing an early stop codon. The mutation was classified as pathogenic in accordance with ACMG classification guidelines. The affected brother carried the same homozygous mutation, and segregation analysis verified that both parents were heterozygous carriers. (Fig. 1)

Family 2: Frameshift Variant (p.Tyr919Serfs*6)

A previously unidentified homozygous frameshift insertion in exon 26 of *DYSF* (c.2755_2756insC; p.Tyr919Serfs*6), which is expected to result in the premature termination of dysferlin protein, was found by WES. According to ACMG criteria, this mutation was categorized as pathogenic. The affected sibling was homozygous for the same mutation, and segregation analysis verified that both parents were heterozygous carriers. (Fig. 2)

Neither variant was present in public population databases such as gnomAD (v4.0.0), indicating their novelty. Segregation analysis via Sanger sequencing confirmed the homozygous status in the affected individuals and the heterozygous carrier status in the unaffected parents in both families (Fig. 1, Fig. 2), consistent with autosomal recessive inheritance. Based on ACMG guidelines, both variants were classified as pathogenic due to the nature of the

truncating mutation, absence from population databases, prediction of pathogenicity by multiple in-silico tools, and the phenotype specificity.

Structural and Conservation Analysis

Multiple sequence alignment obtained from the UCSC Genome Browser confirmed that both affected residues (Glu1802 and Tyr919) were highly conserved across mammalian species (Fig. 1C).

Furthermore, the three-dimensional structures of the dysferlin protein were analyzed using the AlphaFold predicted model retrieved from the Ensembl database. This analysis demonstrated that both variants occurred at critical functional locations:

- The p.Glu1802* variant (Family 1) results in the loss of the entire C-terminal tail and the final C2 domains, which are crucial for calcium-dependent membrane binding and repair.
- The p.Tyr919Serfs*6 variant (Family 2) leads to a major truncation resulting in the loss of DysF and the critical transmembrane domain, severely compromising the protein's ability to anchor to the muscle membrane.

A schematic depiction of the *DYSF* gene structure and the location of these novel variants relative to previously reported pathogenic variants is provided in Fig. 1E. The position of these variants strongly suggests a severe loss-of-function mechanism due to nonsense-mediated decay or the expression of a truncated, non-functional protein.

Exon-Domain Mapping and Distribution of Pathogenic DYSF Variants

With a focus on exons 26 and 46–48, the Table 1 displays the exon-domain mapping of the human *DYSF* canonical transcript (NM_001130987.2) and gathers pathogenic or possibly pathogenic mutations reported in ClinVar, HGMD, and peer-reviewed publications. A portion of the DysF domain, a structurally conserved module essential for dysferlin stability and folding, is represented by exon 26 [10]. Frameshift and loss-of-function changes are often observed in pathogenic mutations in this area, demonstrating the DysF module's high functional sensitivity. On the other hand, sections of the C2E-C2F domains, which are necessary for calcium-dependent membrane contact during sarcolemmal repair, are encoded by exons 46–48 [11]. The functional significance of these C2 domains to dysferlinopathy symptoms is supported by the pathogenic mutations found in these exons, which include missense and nonsense changes affecting conserved residues. This exon-level analysis helps contextualize the novel homozygous mutations identified in our two Families—c.2755_2756insC (p.Tyr919Serfs*6*; exon 26*) and* c.5404G > T (p.Glu1802; exon 47)—by positioning them within recognized mutational hotspots and functional protein modules [12]. **(**Table 1**)**

Table 1
Exon-domain mapping of the human *DYSF* gene and distribution of selected pathogenic variants affecting critical protein regions.

Exon	Amino Acids	Domain	Common Pathogenic/Likely-Pathogenic Variant(s) (HGVS/cDNA)	Mutation Type	Phenotype (Dysferlinopathy)	Reference
25	~ 850–900	Linker before DysF	no well-known recurrent variant	–	–	–
26	~ 901–950	DysF N-terminal region	*c.*2779delG (p.Ala927Leufs*21*) (founder variant in Caucasus Jews)	Frameshift deletion	LGMD2B/Miyoshi myopathy	[13]
27	~ 951–1000	DysF N-terminal region	*c.*2997G > T (p.Trp999Cys) (common variant, milder form)	Missense	Mild LGMD2B/Miyosh (Adolescent onset)	[13]
45	~ 1540–1580	C2E (N-terminal)	*c.*5033G > A (p.Cys1678Tyr)	Missense	LGMD2B (Adult onset)	[14]
46	~ 1581–1670	C2E	no well-known recurrent variant	–	–	–
47	~ 1671–1760	C2E–C2F linker	*c.*5289G > C (p.Glu1763Asp)	Missense	Dysferlinopathy (LGMD2B/Miyoshi)	[15]
48	~ 1761–1850	C2F	*c.*5713C > T (p.Arg1905Ter) (founder variant in Spain)	Nonsense	LGMD2B (severe)	[16]
49	~ 1851–1940	C2F (C-terminal)	no well-known recurrent variant	–	–	–

Comparison of both Families

Similar beginning ages (~ 25 years) and a gradual pattern of proximal muscle weakness, consistent with dysferlinopathy, were seen in both families. The two families' disease severity and pace of progression were comparable; however, Family 2's afflicted sister showed a more advanced clinical stage, probably due to inter-individual variability. Both *DYSF* mutations caused a truncating effect and pathogenic loss of function, even though they involved different exons and mutation types (frameshift versus nonsense).

Discussion

Pathogenic mutations in *DYSF* cause dysferlinopathy, which exhibits a wide range of mutations, including missense, nonsense, frameshift, splice-site changes, and even exon duplications. Critical functional portions of dysferlin, especially its many C2 Ca^{2+}-binding domains, which are essential for membrane resealing and vesicle fusion, are being truncated or otherwise disrupted by numerous known mutations. A preponderance of young-adult onset, usually in the late teens to mid-twenties, and a clinical pattern of progressive proximal (limb-girdle) weakness with significantly elevated muscle enzymes are consistently shown in published cohort and case series from a variety of populations (e.g., Saudi Arabia, Tunisia, China, Switzerland, India, and several multinational investigations) [17].

According to the studies listed in Table 2, The clinical trajectory of dysferlinopathy is diverse, despite some recurring or founder mutations in particular groups. Most series indicate slow to intermediate progression, but individual results vary greatly, and a significant percentage advance to ambulatory loss. Although truncating mutations that impair C2 domains are often linked to functional loss, genotype-phenotype correlations are still imprecise; the same or similar mutations might result in varied degrees of severity among individuals or families. Together, these findings demonstrate the importance of thorough molecular testing, such as whole-exome sequencing, to identify known and unknown *DYSF* mutations, genotype-phenotype relationships, and guide genetic counseling and diagnosis in populations with high consanguinity or population-specific alleles [18, 19].

Table 2
Summary of Cohort Studies on Dysferlinopathy/LGMD Across Diverse Populations

***DYSF* mutation(s)**	**Age of onset**	**Patient cohort**	**Reference**
13 variants (2 compound het); *c.*164_165insA (frameshift) founder	Mean 17.8 y (10–25 y)	53 Saudis (52.8% male; all from Saudi Arabia)	Alharbi et al., *Front. Neurosci.*, 2022 [17]
5 distinct DYSF mutations (Mostly missense)	Median 17 y (IQR 16.8–28.4)	20 Tunisians (Sex ratio 1)	Belhassen et al., *Neuromuscul. Disord.*, 2023 [20]
40 variants (17 missense, 10 nonsense, 7 frameshift, 4 splice, 2 exon dup)	Mean 24.5 y	26 Chinese From 9 provinces; 12F/14M	Wang et al., *BMC Neurol.*, 2022 [18]
Homozygous *c.*3031 + 2T > C (splice) with founder effect; *c.*1064_1065delAA; nonsense *p.Gln957Ter*, *p.Trp1976Ter*	Mean 18.8 y	13 Swiss (6 families; central Switzerland cluster)	Petersen et al., *BMC Neurol.*, 2015 [21]
96 of 125 pts had 2 *DYSF* variants (84 homozygous)	15–26 y	244 Indian (multi-center; mostly adults)	Dastur et al., *Ann. Ind. Acad. Neurol.*, 2017 [19]
~ 175 mutations identified (49% truncating)	Broad (Childhood–adult)	193 international (Jain-funded study across EU, US, Asia)	Harris et al., *Neurol. Genet.*, 2016 [16]

A review of some previously reported dysferlinopathy cases, as summarized in the expanded Table 3, shows that both early-onset and late-onset LGMD resulting from *DYSF* mutations occur across diverse populations and mutation categories. Although truncating variants—including nonsense, frameshift, and splice-site mutations—are more commonly associated with earlier onset, several missense variants have also been reported in early-onset presentations. Conversely, late-onset disease is observed more frequently with missense mutations, yet notable exceptions exist. Importantly, pathogenic variants leading to either early or late onset are distributed throughout multiple C2 domains and across numerous exons, indicating no exon- or domain-specific clustering. Clinically, early-onset cases often demonstrate faster progression and earlier loss of ambulation, whereas late-onset cases generally exhibit milder and more slowly progressive muscle weakness, though considerable phenotypic overlap remains. Population-based comparisons further reveal that identical or similar mutations can appear in different ethnic groups and produce variable ages of onset and progression. Taken together, these findings indicate that there is no strict correlation between mutation type or exon/domain location and the clinical onset of dysferlinopathy. The substantial

phenotypic variability suggests that additional genetic, epigenetic, or environmental modifiers likely contribute to disease onset and progression beyond the primary *DYSF* variant itself [14, 22].

Table 3
Reported DYSF Variants Mapped by Exon/Protein Domain and Their Correlation with Age of Onset (Sorted by Protein Domain & Exon)

Variant (Nucleotide/ Protein)	Age of Onset	Mutation Type	Protein Domain & Exon	Symptoms	Population	Reference
c.895G > T (p.Gly299Trp)	42 (onset), 22 (duration)	Missense	Exon 10	Progressive limb weakness, high CK	UK	(Klinge et al., 2009) [23]
c.1020C > A (p.Ser340Arg)	23 (onset), 13(duration)	Missense	Exon 11	Proximal weakness	UK	(Klinge et al., 2009) [23]
c.1566C > G (p.Tyr522X)	Teens–early adulthood	Nonsense	Exon 16	Lower limb onset, hyperCKaemia	Japanese	(Takahashi et al., 2012)[22]
c.1663C > T (p.Arg555Trp) + c.2997G > T (p.Trp999Cys)	Late 20s	Compound heterozygous missense	Exon 16 & 28	Proximal > distal weakness, upper limb onset	Korean	(Lee et al., 2020)[24]
c.2643 + 2T > C	23 (onset), 13(duration)	Splice site	Intron 24	Proximal weakness, waddling gait, hyperlordosis	UK	(Klinge et al., 2009) [23]
c.2659A > T (p.Lys887X)	20 (onset), 4 (duration)	Nonsense	Exon 26	Progressive limb weakness, high CK	UK	(Klinge et al., 2009) [23]
c.2997G > T (p.Trp999Cys)	Late onset (mean ~ 54 yrs., range 40–60s, homozygotes)	Missense	Exon 28, C2E domain	Proximal > distal weakness, upper limb onset, low CK, no facial weakness	Japanese	(Takahashi et al., 2012)[22]
c.3817-8TG > AA	33 (onset)	Splice site	Exon 32	Progressive limb weakness, high CK	Italian	(K. Kawabe et al.,2004) [25]
c.3517dupT (p.Ser1173PhefsX2)	Not specified	Duplication / Frameshift	Exon 32	Proximal weakness	UK	(Klinge et al., 2009) [23]
c.4010delT	18 (onset)	Frameshift	Exon 38	Proximal > distal weakness, upper limb onset	Chinese	(Li et al., 2020)[26]
c.4200dupC (p.Ile1401HisfsX7)	39 (onset)	Frameshift	Exon 39	Lower limb onset	UK	(Klinge et al., 2009) [23]
c.4497delT	Teens–early adulthood	Frameshift	Exon 41	Lower limb onset	Japanese	(Takahashi et al., 2012)[22]

Variant (Nucleotide/ Protein)	Age of Onset	Mutation Type	Protein Domain & Exon	Symptoms	Population	Reference
c.5033G > A (p.Cys1678Tyr)	57 (onset)	Missense	Exon 45	Progressive limb weakness, high CK	Italian	(Spadafora et al., 2022)[14]
c.5835_5838del (p.Gln1946TrpfsX18)	22 (onset)	Deletion/ Frameshift	Exon 53	Proximal weakness	US	(Kesari et al., 2008) [14]

In this report, we presented two unrelated siblings with limb-girdle muscular dystrophy that carried two novel homozygous *DYSF* mutations: one frameshift insertion (p.Tyr919Serfs*6) in exon 26 and one nonsense (p.Glu1802*) in exon 47. The mutational spectrum of *DYSF* is expanded since, to the best of our knowledge, neither mutation has previously been reported in significant population or illness databases, such as gnomAD, ClinVar, or HGMD.

Some additional hereditary myopathies must be carefully distinguished from the clinical manifestation of progressive proximal muscle weakening, high serum CK values, and an adult-onset course. Although Becker muscular dystrophy (BMD) is commonly connected to X-linked inheritance, pseudohypertrophy of calf muscles, and dystrophin deficiency on biopsy—features not seen in our patients—it may exhibit a similar limb-girdle pattern of weakening [27]. Another important differential diagnosis is anoctaminopathy caused by ANO5 mutations, especially in cases of adult-onset limb-girdle weakness with noticeably increased CK. However, asymmetric involvement and particular patterns on muscle MRI are common in ANO5-related myopathy, which were not reported here [27]. Although it frequently exhibits early scapular winging, Achilles tendon contractures, and distinctive findings on muscle biopsy, calpainopathy (LGMDR1, caused by CAPN3 mutations) also share clinical similarities with dysferlinopathy. The absence of these distinguishing features, combined with clear segregation of pathogenic mutations in *DYSF*, supports dysferlinopathy as the most plausible diagnosis in these Families [27].

Both index patients had a similar pattern of increasing proximal muscle weakness and a similar beginning age in their mid-twenties. Based on available clinical data, the overall progression rate in both families was roughly equivalent, despite the affected sister of family 2 appearing to have somewhat more advanced clinical severity. For properly understanding inter-individual variability, a characteristic of dysferlinopathies, long-term follow-up is required. In line with the high frequency of *DYSF*-related myopathies in populations with consanguineous marriages, segregation analysis verified autosomal recessive inheritance in both families. The significance of genetic counseling in communities with high consanguinity rates is highlighted by the existence of affected siblings in both families.

One of the main strengths of our study is the use of WES, which was essential to the diagnosis. Due to the clinical overlap between dysferlinopathies and other limb-girdle muscular dystrophy subtypes and the absence of muscle biopsy or MRI data, WES was a crucial diagnostic method that enabled the timely identification of causative mutations. This illustrates the growing importance of NGS in evaluating undiscovered myopathies, particularly in settings where access to advanced neuropathology or imaging is limited. In addition to helping to define the disease subtype and prognosis, early molecular diagnosis guides genetic counseling, carrier screening, and reproductive decision-making [28].

Finally, our results confirm the diagnostic utility of WES in LGMDs, especially in populations with high consanguinity, and expand the range of pathogenic *DYSF* mutations. Recurrence prevention in families at-risk can be greatly aided by early genetic testing and counseling, which are still crucial elements of patient care.

Despite the remarkable molecular findings, this work has limitations linked to retrospective data gathering in rare genetic illnesses. Due in large part to restricted access to specialist facilities and the high expense of invasive testing, we were unable to get a muscle sample with dysferlin immunohistochemistry or a thorough muscle MRI. The discovery of two novel homozygous pathogenic mutations and their obvious co-segregation in both consanguineous families—supported by in-silico predictions and structural analysis—provides strong evidence consistent with ACMG pathogenicity criteria, even though these complementary data strengthened clinical confirmation. To better understand the biological effects of these mutations on dysferlin's membrane-repair function, more functional research is required [28].

Conclusion

In two separate families with dysferlinopathy, WES effectively detected two unique pathogenic variants in the *DYSF* gene: one frameshift (c.2755_2756insC; p.Tyr919Serfs*6) and one nonsense (c.5404G > T; p.Glu1802*). In each family, both mutations were homozygous and segregated with disease, which is consistent with autosomal recessive inheritance.

Similar clinical features, such as proximal muscle weakening, elevated muscle enzymes, and a progressive course starting in their mid-20s, were present in all affected patients. Our findings highlight the critical diagnostic use of WES, especially in populations where novel mutations are more prevalent due to consanguineous marriages. Early genetic diagnosis enables appropriate clinical therapy, accurate genetic counseling, and informed family planning. Further long-term clinical surveillance and functional studies are needed to fully comprehend how these particular *DYSF* mutations impact dysferlin structure and function.

Abbreviations

ACMG American College of Medical Genetics and Genomics

BMD Becker muscular dystrophy

EMG electromyography

LGMDR2 limb-girdle muscular dystrophy type R2

LGMDs limb-girdle muscular dystrophies

WES Whole-exome sequencing

Declarations

Ethics approval and consent to participate

This study was conducted in accordance with the Declaration of Helsinki and was approved by the Ethics Committee of Shiraz University of Medical Sciences, Shiraz, Iran (Ethics approval code: IR.SUMS.MED.REC.1404.188). Written informed consent was obtained from all participants prior to enrollment.

Consent for publication

Written informed consent for physical examination, molecular investigation, and publication of the results was obtained.

Competing interests

The authors declare that they have no competing interests.

Funding

This study was financially supported by Shiraz University of Medical Sciences (grant number: 32426). The funders have no role in the study design, data collection, analyses, decision to publish, or manuscript writing.

Author Contribution

Y.Z. contributed to the conception and design of the study, acquisition of data, analysis and interpretation of data, and drafting of the original manuscript. M.F.H. contributed to data acquisition, analysis and interpretation of data, and critical revision of the manuscript for important intellectual content. Z.F. contributed to data acquisition and drafting of the manuscript. F.J. contributed to data acquisition and drafting of the manuscript. E.K. contributed to data acquisition and drafting of the manuscript. J.M.S. contributed to the conception and design of the study, supervision of the project, data acquisition, analysis and interpretation of data, and critical revision of the manuscript. All authors read and approved the final version of the manuscript to be submitted and agree to be accountable for all aspects of the work.

Acknowledgement

The authors would like to thank Shiraz University of Medical Sciences, Shiraz, Iran, and also Center for Development of Clinical Research of Nemazee Hospital, and Dr. Nasrin Shokrpour for editorial assistance.

Data Availability

The raw whole-exome sequencing (WES) data generated and analysed during the current study have been deposited in the NCBI Sequence Read Archive (SRA) under BioProject accession number PRJNA1522894. The raw Sanger chromatogram files (.ab1) supporting variant confirmation and segregation analysis in the two families are available in the Zenodo repository at https://doi.org/10.5281/zenodo.22286007.

References

1. Jin SQ, Yu M, Zhang W, Lyu H, Yuan Y, Wang ZX. Dysferlin Gene Mutation Spectrum in a Large Cohort of Chinese Patients with Dysferlinopathy. Chin Med J (Engl). 2016;129(19):2287-93. http://doi.org/10.4103/0366-6999.190671.
2. Bouchard C, Rousseau J, Lamothe G, Dubost M, Bastrenta L, Ramezani S, et al. In Vitro Correction of Point Mutations in the DYSF Gene Using Prime Editing. Int J Mol Sci. 2025;26(12). http://doi.org/10.3390/ijms26125647.
3. Paulke NJ, Fleischhacker C, Wegener JB, Riedemann GC, Cretu C, Mushtaq M, et al. Dysferlin Enables Tubular Membrane Proliferation in Cardiac Hypertrophy. Circ Res. 2024;135(5):554-74. http://doi.org/10.1161/circresaha.124.324588.

4. Charnay T, Blanck V, Cerino M, Bartoli M, Riccardi F, Bonello-Palot N, et al. Retrospective analysis and reclassification of DYSF variants in a large French series of dysferlinopathy patients. Genet Med. 2021;23(8):1574-7. http://doi.org/10.1038/s41436-021-01164-3.
5. Fichna JP, Macias A, Piechota M, Korostyński M, Potulska-Chromik A, Redowicz MJ, et al. Whole-exome sequencing identifies novel pathogenic mutations and putative phenotype-influencing variants in Polish limb-girdle muscular dystrophy patients. Hum Genomics. 2018;12(1):34. http://doi.org/10.1186/s40246-018-0167-1.
6. Beekman C, Janson AA, Baghat A, van Deutekom JC, Datson NA. Use of capillary Western immunoassay (Wes) for quantification of dystrophin levels in skeletal muscle of healthy controls and individuals with Becker and Duchenne muscular dystrophy. PLoS One. 2018;13(4):e0195850. http://doi.org/10.1371/journal.pone.0195850.
7. Tiwari A, Lemke J, Altmueller J, Thiele H, Glaus E, Fleischhauer J, et al. Identification of Novel and Recurrent Disease-Causing Mutations in Retinal Dystrophies Using Whole Exome Sequencing (WES): Benefits and Limitations. PLoS One. 2016;11(7):e0158692. http://doi.org/10.1371/journal.pone.0158692.
8. Green RC, Berg JS, Grody WW, Kalia SS, Korf BR, Martin CL, et al. ACMG recommendations for reporting of incidental findings in clinical exome and genome sequencing. Genet Med. 2013;15(7):565-74. http://doi.org/10.1038/gim.2013.73.
9. McCormick JB, Sharp RR, Farrugia G, Lindor NM, Babovic-Vuksanovic D, Borad MJ, et al. Genomic medicine and incidental findings: balancing actionability and patient autonomy. Mayo Clin Proc. 2014;89(6):718-21. http://doi.org/10.1016/j.mayocp.2014.04.008.
10. Urtizberea JA, Bassez G, Leturcq F, Nguyen K, Krahn M, Levy N. Dysferlinopathies. Neurol India. 2008;56(3):289-97. http://doi.org/10.4103/0028-3886.43447.
11. Ivanova A, Smirnikhina S, Lavrov A. Dysferlinopathies: Clinical and genetic variability. Clin Genet. 2022;102(6):465-73. http://doi.org/10.1111/cge.14216.
12. Barthélémy F, Wein N, Krahn M, Lévy N, Bartoli M. Translational research and therapeutic perspectives in dysferlinopathies. Mol Med. 2011;17(9-10):875-82. http://doi.org/10.2119/molmed.2011.00084.
13. Argov Z, Sadeh M, Mazor K, Soffer D, Kahana E, Eisenberg I, et al. Muscular dystrophy due to dysferlin deficiency in Libyan Jews. Clinical and genetic features. Brain. 2000;123 (Pt 6):1229-37. http://doi.org/10.1093/brain/123.6.1229.
14. Spadafora P, Qualtieri A, Cavalcanti F, Di Palma G, Gallo O, De Benedittis S, et al. A novel homozygous variant in DYSF gene is associated with autosomal recessive limb girdle muscular dystrophy R2/2B. Int J Mol Sci. 2022;23(16):8932. http://doi.org/10.3390/ijms23168932.
15. Meznaric M, Gonzalez-Quereda L, Gallardo E, de Luna N, Gallano P, Fanin M, et al. Abnormal expression of dysferlin in skeletal muscle and monocytes supports primary dysferlinopathy in patients with one mutated allele. Eur J Neurol. 2011;18(7):1021-3. http://doi.org/10.1111/j.1468-1331.2010.03240.x.
16. Harris E, Bladen CL, Mayhew A, James M, Bettinson K, Moore U, et al. The clinical outcome study for dysferlinopathy: an international multicenter study. Neurol Genet. 2016;2(4):e89. http://doi.org/10.1212/NXG.0000000000000089.
17. Alharbi N, Matar R, Cupler E, Al-Hindi H, Murad H, Alhomud I, et al. Clinical, Neurophysiological, Radiological, Pathological, and Genetic Features of Dysferlinopathy in Saudi Arabia. Front Neurosci. 2022;16:815556. http://doi.org/10.3389/fnins.2022.815556.
18. Wang N, Han X, Hao S, Han J, Zhou X, Sun S, et al. The clinical, myopathological, and molecular characteristics of 26 Chinese patients with dysferlinopathy: a high proportion of misdiagnosis and novel variants. BMC Neurology. 2022;22(1):398. http://doi.org/10.1186/s12883-022-02905-w.

19. Dastur RS, Gaitonde PS, Kachwala M, Nallamilli BRR, Ankala A, Khadilkar SV, et al. Detection of Dysferlin Gene Pathogenic Variants in the Indian Population in Patients Predicted to have a Dysferlinopathy Using a Blood-based Monocyte Assay and Clinical Algorithm: A Model for Accurate and Cost-effective Diagnosis. Annals of Indian Academy of Neurology. 2017;20(3):302-8. http://doi.org/10.4103/aian.AIAN_129_17.
20. Belhassen I, Laroussi S, Sakka S, Rekik S, Lahkim L, Dammak M, et al. Dysferlinopathy in Tunisia: clinical spectrum, genetic background and prognostic profile. Neuromuscul Disord. 2023;33(10):718-27. http://doi.org/10.1016/j.nmd.2023.08.007.
21. Petersen JA, Kuntzer T, Fischer D, von der Hagen M, Huebner A, Kana V, et al. Dysferlinopathy in Switzerland: clinical phenotypes and potential founder effects. BMC Neurology. 2015;15(1):182. http://doi.org/10.1186/s12883-015-0449-3.
22. Takahashi T, Aoki M, Suzuki N, Tateyama M, Yaginuma C, Sato H, et al. Clinical features and a mutation with late onset of limb girdle muscular dystrophy 2B. Journal of Neurology, Neurosurgery & Psychiatry. 2013;84(4):433-40. http://doi.org/10.1136/jnnp-2011-301339.
23. Klinge L, Aboumousa A, Eagle M, Hudson J, Sarkozy A, Vita G, et al. New aspects on patients affected by dysferlin deficient muscular dystrophy. J Neurol Neurosurg Psychiatry. 2010;81(9):946-53. http://doi.org/10.1136/jnnp.2009.178038.
24. Lee SJ, Choi E, Shin S, Park J. Genetically confirmed limb-girdle muscular dystrophy type 2B with DYSF mutation using gene panel sequencing: A case report. Medicine. 2020;99(28):e20810. http://doi.org/10.1097/md.0000000000020810.
25. Kawabe K, Goto K, Nishino I, Angelini C, Hayashi YK. Dysferlin mutation analysis in a group of Italian patients with limb-girdle muscular dystrophy and Miyoshi myopathy. European Journal of Neurology. 2004;11(10):657-61. http://doi.org/https://doi.org/10.1111/j.1468-1331.2004.00755.x.
26. Li Q, Tan C, Chen J, Zhang L. Next-generation sequencing identified a novel DYSF variant in a patient with limb-girdle muscular dystrophy type 2B: A case report. Medicine. 2020;99(41):e22615. http://doi.org/10.1097/md.0000000000022615.
27. Magot A, Wahbi K, Leturcq F, Jaffre S, Péréon Y, Sole G. Diagnosis and management of Becker muscular dystrophy: the French guidelines. J Neurol. 2023;270(10):4763-81. http://doi.org/10.1007/s00415-023-11837-5.
28. Fanin M, Angelini C. Progress and challenges in diagnosis of dysferlinopathy. Muscle Nerve. 2016;54(5):821-35. http://doi.org/10.1002/mus.25367.

Figures

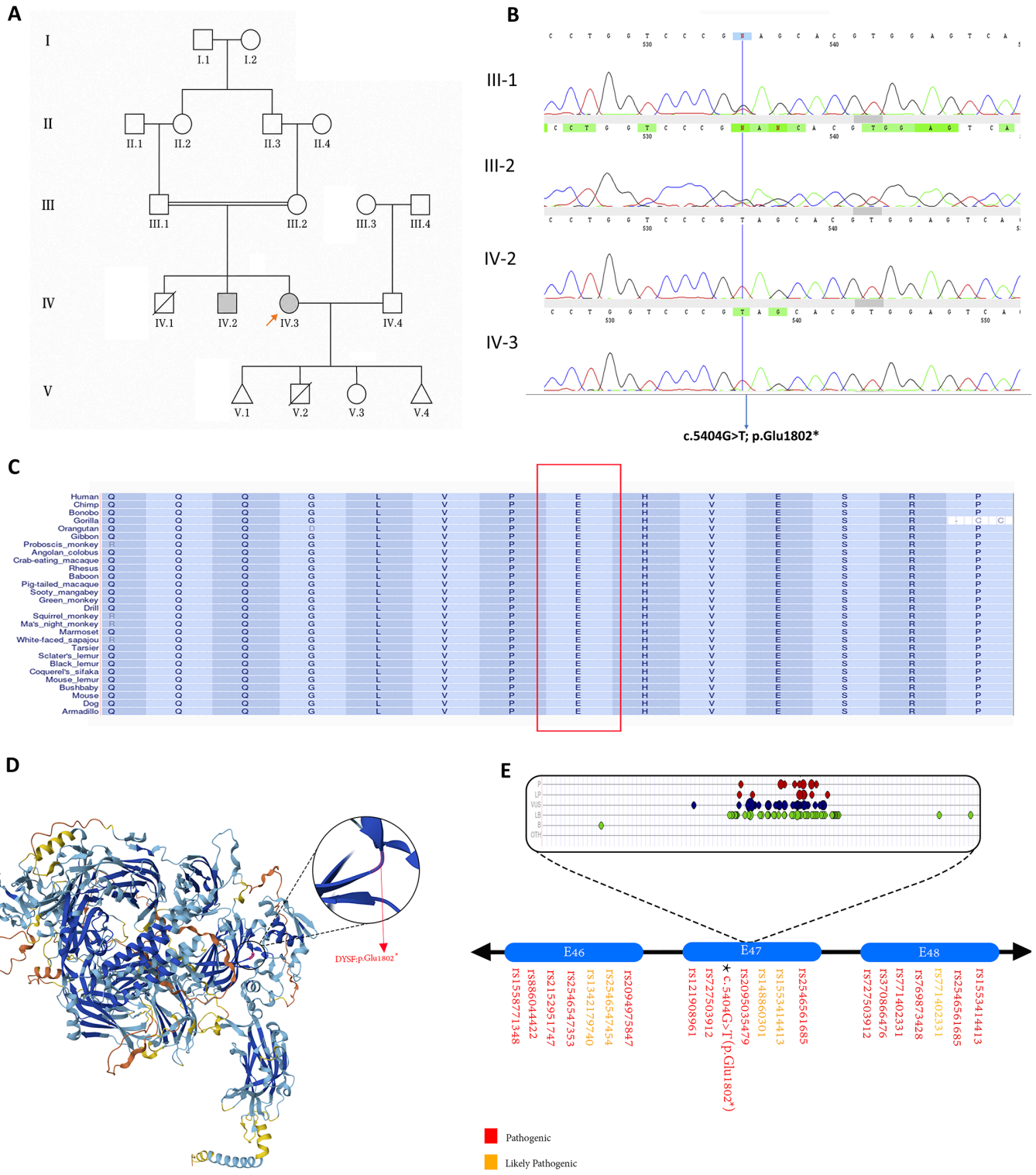


Figure 1

Pedigree, electropherograms, conservation analysis, and structural modeling of the *DYSF* variant. A: Family pedigree; the index patient is marked with a black arrowhead. **B:** Electropherograms of parents (III-1, III-2), affected brother (IV-2), and index patient (IV-3), confirming segregation of the *DYSF* c.5404G>T variant. **C:** Multiple sequence alignment from UCSC Genome Browser, demonstrating conservation of the Glutamic acid residue at position 1802 (red box). **D:** AlphaFold-predicted 3D structure of dysferlin protein (from Ensembl), showing location of p.Glu1802* variant. **E:**

Schematic representation of *DYSF* exons 46-48 and distribution of neighboring pathogenic variants based on UCSC Genome Browser data; the star indicates the novel nonsense variant identified in this investigation.

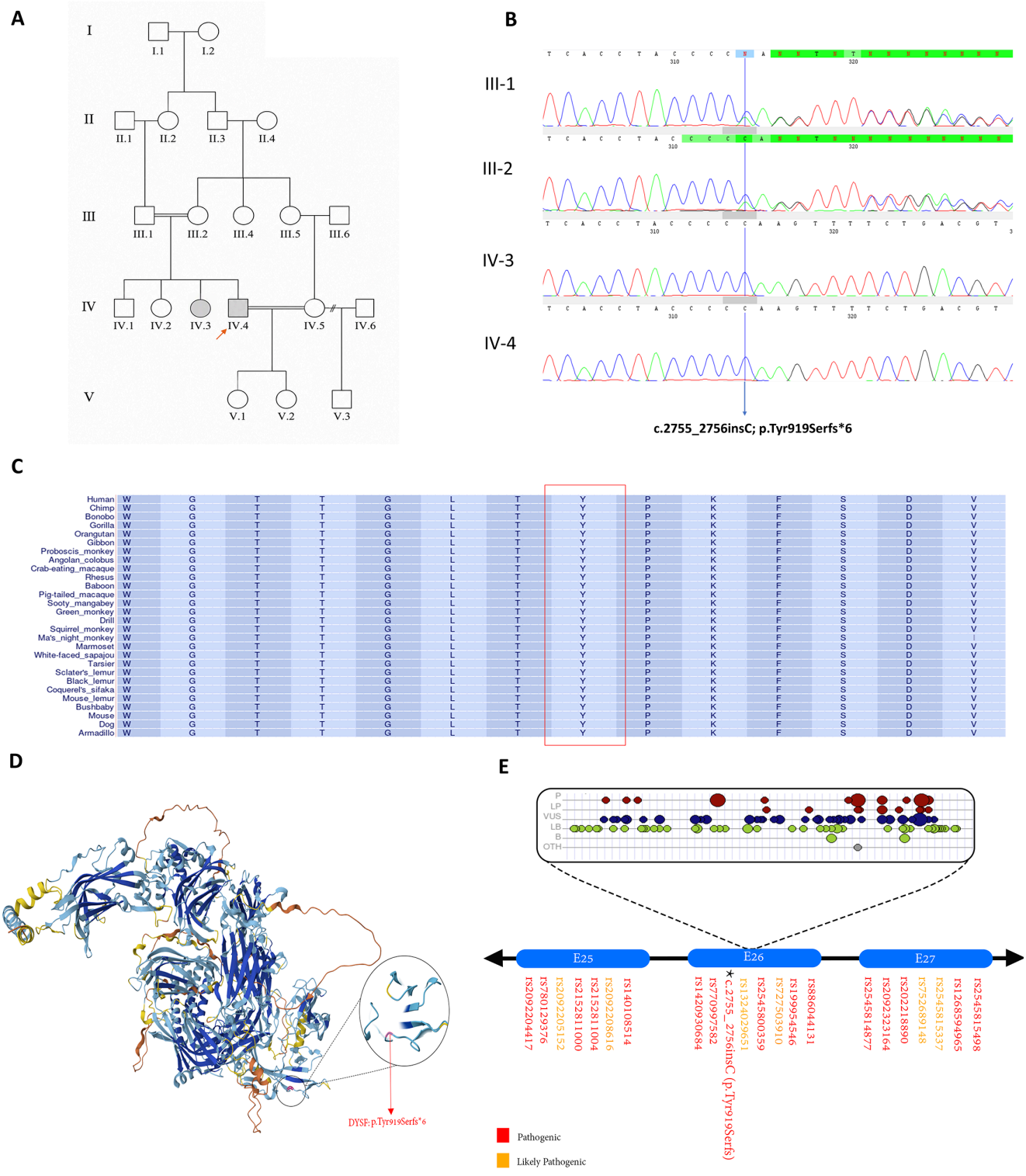


Figure 2

Genetic characterization and structural analysis of the novel *DYSF* variant. A: Family pedigree showing segregation pattern, with index patient (IV-4) indicated by black arrowhead. **B:** Sanger sequencing chromatograms of family members confirming segregation of *DYSF* frameshift variant, c.2755_2756delC (p.Tyr919Serfs6), electropherograms

of parents (III-1, III-2), affected sister (IV-3), and index patient (IV-4). **C:** Multiple sequence alignment from UCSC Genome Browser, demonstrating evolutionary conservation of Tyrosine residue (Y) at codon 919 (red box). **D:** AlphaFold-predicted 3D structure of dysferlin protein (from Ensembl), highlighting position of novel frameshift variant (p.Tyr919Serfs6). **E:** Schematic representation of *DYSF* exons 25-27 and distribution of neighboring pathogenic variants based on UCSC Genome Browser data; the star denotes the novel frameshift variant identified in this study, while other pathogenic (red) and likely pathogenic (orange) variants are displayed for comparison.